Cement & Concrete Composites 32 (2010) 34–42

Contents lists available at ScienceDirect

Cement & Concrete Composites

journal homepage: www.elsevier.com/locate/cemconcomp

Chloride resistance of concrete and its binding capacity – Comparison between experimental results and thermodynamic modeling

Roman Loser *, Barbara Lothenbach, Andreas Leemann, Martin Tuchschmid

Empa, Swiss Federal Laboratories for Materials Testing and Research, Switzerland

ARTICLE INFO

Article history:
Received 27 March 2009
Received in revised form 10 August 2009
Accepted 10 August 2009
Available online 14 August 2009

Keywords:
Concrete
Chloride resistance
Chloride binding
Thermodynamic modeling
Mineral admixtures

ABSTRACT

The chloride resistance of concrete mixtures produced with different binders and water-to-binder ratios is determined by three different methods (natural chloride diffusion, accelerated chloride migration and conductivity measurement). The influence of mix design and type of binder are evaluated and related to porosity. The effect of chloride binding on chloride resistance is assessed by thermodynamic modeling and compared with chloride content measured with acid and water extraction.

Chloride resistance depends on the type of binder and on water-to-binder ratio. Chloride content measurements and thermodynamic modeling both show that chloride binding is strongly related to the hydration degree of the cement and of the mineral admixtures. However, the decisive parameter for chloride resistance in all the tests is the permeability while the influence of chloride binding is less important.

1. Introduction

Resistance of concrete to chloride ingress is a key property for the durability of reinforced concrete structures exposed to de-icing salts or sea water. If chloride penetrates into concrete, it can cause fast and severe corrosion of the reinforcement [1] which reduces the cross-section of the reinforcement and thus leads to the loss of its load carrying capacity. Chloride induced corrosion of the reinforcement is one of the main causes of structural concrete deterioration and therefore responsible for a large share of the cost for the rehabilitation of concrete structures [2]. The thickness of concrete cover over the reinforcement and the permeability of the concrete are used to control the ingress of chloride to prevent corrosion in reinforced concrete structures.

For this reason, chloride penetration into concrete has been investigated for many years. It is known that cement has the ability to bind chlorides, dependent on its chemical composition. Therefore, chloride is present in concrete both as ion in the pore solution as well as bound to cement hydration products in the form of Friedel's salt ($Ca_4Al_2Cl_2(OH)_{12}\cdot 4H_2O$) or sorbed to C–S–H [3–5]. Since only "free" chloride ions in the pore solution can move, chloride binding can affect resistance of concrete to chloride ingress by delaying the penetration process. So far, chloride binding has been mainly studied using experimental techniques. Few attempts have been made to investigate the subject by thermodynamic modeling [6,7]. Additionally, the chloride resistance of a cement based material is known to increase with decreasing porosity [8,9] since the mobility of water and thus of the chloride ions is reduced.

To characterize the resistance of concrete against chloride ingress numerous tests have been developed. An overview of such test methods is given e.g. in [10,11]. These methods can mainly be categorized into three categories: diffusion tests, migration tests and indirect tests based on resistivity or conductivity.

In diffusion tests, chloride penetrates slowly into the saturated concrete due to a gradient in chloride concentration, while in the migration and indirect tests, the chloride transport is accelerated by an externally applied electrical field. Furthermore, the difference between steady-state and non-steady-state testing conditions have to be distinguished.

Under steady-state testing conditions (e.g. conductivity tests), the extent of chloride binding has no influence on the results. However, non-steady-state transport can be affected by chloride binding, dependent on the method used. Non-steady-state migration tests are working with a strong external electrical field and a shorter test duration than non-steady-state diffusion tests, which both tend to reduce the amount of bound chlorides. Therefore, non-steady-state migration coefficient describes chloride transport under reduced chloride binding conditions [12]. As a result, the different test methods may lead to results which are not comparable to each other.

The aim of this study is to investigate the influence of permeability and chloride binding on chloride resistance of concrete by combining experimental techniques with thermodynamic modeling.

* Corresponding author. Address: Laboratory for Concrete/Construction Chemistry, Empa, Swiss Federal Laboratories for Materials Testing and Research, Überlandstrasse 129, 8600 Dübendorf, Switzerland. Tel.: +41 44 823 42 35.
E-mail address: roman.loser@empa.ch (R. Loser).

0958-9465/$ - see front matter © 2009 Elsevier Ltd. All rights reserved.
doi:10.1016/j.cemconcomp.2009.08.001

The chloride resistance of concrete produced with different binders is measured using a rapid migration test, a diffusion test and a conductivity test. Furthermore, the influences of mix design and type of binder are evaluated and related to porosity. The importance of chloride binding on the results is assessed by combining chloride content measurements (using acid and water extraction) with thermodynamic modeling.

2. Specimen production

2.1. Materials

Four different types of binder according to European standard EN 197-1 [13] were used (Table 1). While CEM I is an ordinary Portland cement (OPC), CEM II/A-LL and CEM III/A are industrially mixed binders containing 80–94% OPC and 6–20% limestone powder for CEM II/A-LL and 35–64% OPC and 36–65% slag for CEM III/A, respectively. The precise amount of industrially replaced OPC by limestone powder and slag is not known. For the modeling a limestone content of 14% and slag content of 65% was used. A low CaO fly ash (V) was used additionally to blend it with the OPC during concrete mixing in the lab. The fly ash replaced OPC by 20% by weight.

As aggregate natural sand and gravel with a high percentage of well-rounded particles was used. The maximum grain size was 32 mm for conventionally vibrated concrete (CVC) and 16 mm for self-compacting concrete (SCC). Workability was controlled using a polycarboxylate type superplasticizer (SP).

2.2. Mixtures and specimens

Three CVC-mixtures with variable water-to-binder ratio (w/b = 0.35, 0.45, 0.60) and constant volume of paste and one SCC-mixture with w/b = 0.40 were produced with every binder (Table 2). The volume of paste of SCC is about 75 l/m^3 higher compared to the one of CVC and as a result contains less aggregate. The workability of SCC was determined by measuring flow (without knocking) and flow time in the L-box [14]. For CVC flow was measured according to [15].

After production, the test specimens (prisms $120 \times 120 \times 360$ mm^3 and cubes $150 \times 150 \times 150$ mm^3) for all tests were stored at 20 °C and 90% relative humidity (r.h.) for 24 h. Afterwards, they were demolded and stored in saturated calcium hydroxide solution for 62 days to reduce the influence of ongoing hydration on the test results. Immediately after storage, the specimens for the different chloride resistance tests were cut out of the prisms and the testing procedure was started.

3. Test methods

3.1. Compressive strength

Compressive strength of the different mixtures was determined on cubes according to [16] as the average of three specimens at the age of 63 days.

3.2. Chloride resistance

Chloride resistance was measured using three different methods; two of the methods characterize non-steady-state and the other steady-state conditions:

– Natural diffusion test according to ASTM C 1556 [17] on saturated specimens (cubes $120 \times 120 \times 120$ mm^3 cut out of the prisms) with an immersion duration of 50 days in a concentrated chloride solution (165 g NaCl per liter solution) leading

Table 1
Types of binder named according to EN 197-1 and their chemical composition (LOI = loss on ignition).

Type (–)	Abbrev. (–)	CaO (%)	SiO_2 (%)	Al_2O_3 (%)	Fe_2O_3 (%)	MgO (%)	K_2O (%)	Na_2O (%)	SO_3 (%)	Blaine (cm^2/g)	LOI (%)	Density (kg/m^3)
CEM I 42.5 N	CEM I	60.9	19.2	5.3	3.1	2.0	1.2	0.2	3.1	2990	2.7	3140
CEM II/A-LL 42.5 N	CEM II	62.8	17.7	4.2	2.3	1.6	0.9	0.1	2.8	4320	7.2	3070
CEM III/A 32.5 N	CEM III	50.8	27.3	7.1	1.7	4.0	1.0	0.1	2.8	4130	1.8	2990
Fly ash	V	1.9	56.0	25.0	8.7	3.1	3.3	0.2	0.0	2370	2.2	2130

Table 2
Composition and workability of the SCC- and CVC-mixtures (agg: aggregate, s/g: sand/gravel-ratio, w/b: water/binder-ratio, SP: superplasticizer). Indication of the mixtures: concrete type (C = CVC, S = SCC), cement type, w/b. Example: C1 V-45 = CVC with CEM I and fly ash and w/b of 0.45.

Mixture (–)	Agg. (kg/m^3)	s/g (–)	CEM I (kg/m^3)	CEM II (kg/m^3)	CEM III (kg/m^3)	V (kg/m^3)	Water (kg/m^3)	w/b (–)	SP (kg/m^3)	Vol. of paste (l/m^3)	Flow (cm)	L-box (s)
C1-35	1930	0.54	375	–	–	–	131	0.35	4.88	257	46	–
C1-45	1933	0.54	330	–	–	–	149	0.45	1.65	256	47	–
C160	1928	0.54	280	–	–	–	168	0.60	0.00	257	57	–
S1-40	1735	1.00	455	–	–	–	178	0.40	7.28	330	62	4.2
C2-35	1931	0.54	–	371	–	–	130	0.35	5.57	256	49	–
C2-45	1934	0.54	–	327	–	–	147	0.45	1.64	255	49	–
C2-60	1928	0.54	–	278	–	–	167	0.60	0.00	257	53	–
S2-40	1735	1.00	–	451	–	–	177	0.40	6.32	330	64	2.2
C1 V-35	1930	0.54	290	–	–	73	127	0.35	5.44	257	47	–
C1 V-45	1934	0.54	256	–	–	64	144	0.45	1.60	255	48	–
C1 V-60	1929	0.54	218	–	–	55	164	0.60	0.00	257	57	–
S1 V-40	1734	1.00	353	–	–	88	173	0.40	6.18	331	64	3.4
C3-35	1930	0.54	–	–	367	–	128	0.35	3.24	257	42	–
C3-45	1932	0.54	–	–	324	–	146	0.45	0.81	256	42	–
C3-60	1938	0.54	–	–	278	–	160	0.58	0.00	258	53	–
S3-40	1735	1.00	–	–	446	–	175	0.40	4.46	330	68	3.4

to an *apparent chloride diffusion coefficient* D_i (non-steady-state) by fitting chloride profiles to the error-function solution to Fick's second law.
- Rapid chloride migration test according to Swiss standard SIA 262/1 [18] with a test duration of 24 h at an externally applied potential of 20 V leading to a *chloride migration coefficient* D_m (non-steady-state) calculated from penetration depth of chlorides (colorimetric determination). During the test, one surface of the saturated test specimen (cores with diameter and length of 50 mm) is exposed to a 0.2 M potassium hydroxide solution without chlorides while the potassium hydroxide solution in contact with the second surface contains 3% NaCl.
- Rapid chloride conductivity test described in [19] measured using samples (cores with diameter of 68 mm and length of 25 mm) saturated with 5 M chloride solution with an externally applied potential of 10 V leading to a *conductivity* σ (steady-state) calculated from the measured current.

3.3. Chloride binding

The chloride binding capacity of the different binders was evaluated as the difference between the acid-soluble and the water-soluble chloride content following European standard EN 14629 [20], with the only difference in dilution solution being water or diluted nitric acid. The water-soluble chloride content was determined at selected samples which were taken from the same powders used for the acid-soluble chloride content profiles in the test ASTM C 1556 after 50 days immersion. The samples selected for analysis were all mixtures with CEM I as binder (C1-35, -45, -60 and S1-40) and the CVC-mixtures of the other binders with a w/b of 0.45. Note that for the following discussion the chloride content determined with diluted nitric acid is defined as the total chloride content whereas the water-soluble chloride content is defined as the free chloride content. The results are expressed as mass% chlorides per mass of unit cement in each mixture proportion.

One has to be aware that, contrary to the reference method for determining free chloride content (mass%/cement) by analyzing expressed pore solution from uncrushed samples, bound chlorides can also be extracted by dissolving the chlorides with water. But, as shown in a Round-Robin test [21], the free chloride content can be determined reasonably rigorously if the contact time between water and crushed concrete sample lasts a short time (here 5 min). Moreover, the results presented in this paper are used for a relative comparison between different binders only and not as absolute values. Therefore, this procedure of obtaining free chloride content should be accurate enough for using the results as a basis to asses the influence of chloride binding on the test results and for comparison to thermodynamic modeling.

3.4. Porosity

Pore characteristics were determined using mercury intrusion porosimetry (MIP). Several samples with aggregate diameters <2 mm were cut with pincers from every concrete mixture at the age of 63 days. Afterwards, the pieces were stored in isopropanol for 7 days and then dried at 50 °C for another 7 days. After this conditioning MIP was determined using a Thermoelectron Pascal 140/440 equipment with a maximum pressure of p_{max} = 395 MPa.

3.5. Thermodynamic modeling

Thermodynamic modeling was used to study the chemical changes (formation of Friedel's salt) associated with the ingression of chloride in the different cement types. Thermodynamic modeling was carried out using the Gibbs free energy minimization program GEMS [22]. GEMS is a broad-purpose geochemical modeling code which computes equilibrium phase assemblage and speciation in a complex chemical system from its total bulk elemental composition. Chemical interactions involving solids, solid solutions, and aqueous electrolyte are considered simultaneously. The speciation of the dissolved species as well as the kind and amount of solids precipitated are calculated.

The thermodynamic data for aqueous species, gaseous phases as well as for many solids were taken from the PSI-GEMS thermodynamic database [23,24]. Solubility products for cement minerals including ettringite, different AFm phases, hydrogarnet, C–S–H and hydrotalcite were taken from the recent cemdata07 compilation [25]. The extent of the reaction of the clinker phases has been assumed according to the data presented previously [26], taking a total hydration time of 110 days for all concrete samples in accordance with the total hydration time of the samples in the ASTM test (63 days of curing + 50 days of test). For the small amount of ferrite reacted, the formation of Fe-hydroxide was assumed.

The reaction of chloride with Al-bearing phases was considered by using a solubility product of −27.3 for the reaction $Ca_4Al_2Cl_2(OH)_{12}\cdot 4H_2O \rightarrow 4Ca^{2+} + 2Al(OH)_4^- + 4OH^- + 2Cl^- + 4H_2O$, fitted based on the solubility data measured by Hobbs [27]. An ideal solid between Friedel's salt – C_4AH_{13} and Friedel's salt – monocarbonate was considered.

Thermodynamic modeling can be used to calculate the changes associated with the ingression of NaCl in a concrete sample. The different conditions which may be present throughout a concrete sample submersed in NaCl solutions can be expressed as a function of ml NaCl solution, assuming that in the core of the sample, basically no additional NaCl solution is present, while the binder directly at the surface is in contact with a relatively large volume of NaCl solution. Thus as x-axis the quantity of NaCl solution in contact with a specific amount (e.g. 100 g) of the binder is used. In all calculations a solution with 165 g NaCl per liter solution was used, in accordance to the concentration used in the ASTM test. Such a modeling approach has the advantage that the calculations are very fast and flexible as no transport equations have to be considered, but has the disadvantage that the calculated data relate neither to time nor to distance.

4. Results and discussion

A summary of compressive strength, porosity and results of chloride resistance is given in Table 3.

4.1. Compressive strength

Compressive strength is negatively correlated with the w/b and is comparable between the different binders at constant w/b. The CVC-mixtures with the highest w/b (0.60) have a compressive strength which is about half of the strength obtained with the lowest w/b (0.35). The compressive strength of SCC slightly exceeds the w/b-to-strength relation established with CVC for a particular binder.

4.2. Porosity MIP

Total porosity determined by MIP is increasing linearly with increasing w/b (Fig. 1). However, the slope is steeper for CEM II than for the other binders. At constant w/b, the difference in total porosity between the different binders is rather small compared to the influence of a change in w/b. Total porosity of SCC is slightly higher than for CVC, which is a result of the higher volume of paste for SCC. The pore size distribution determined by MIP based on the

Table 3
Results of the different measurements for all concrete mixtures measured at the age of 63 days.

Mixture (–)	Compressive strength (MPa)	Total porosity MIP (mm^3/g)	D_i ($\times 10^{-12}$ m^2/s)	D_m ($\times 10^{-12}$ m^2/s)	σ (ms/cm)
C1-35	84.1	36	1.6	1.3	–
C1-45	65.1	49	2.9	5.6	–
C1-60	42.1	65	5.7	11.3	–
S1-40	77.3	42	2.2	4.4	–
C2-35	81.3	32	3.1	5.7	0.42
C2-45	60.5	50	6.6	9.9	0.66
C2-60	44.5	76	7.9	18.8	1.50
S2-40	74.9	48	4.6	7.9	–
C1 V-35	85.9	40	1.4	1.8	0.22
C1 V-45	67.6	54	2.5	5.4	0.45
C1 V-60	41.2	72	5.3	9.6	0.91
S1 V-40	78.5	50	1.7	3.0	–
C3-35	85.1	37	0.9	0.2	0.16
C3-45	60.7	50	1.1	1.0	0.22
C3-60	48.4	68	1.0	1.8	0.33
S3-40	82.1	52	0.6	0.3	–

– = Not analyzed.

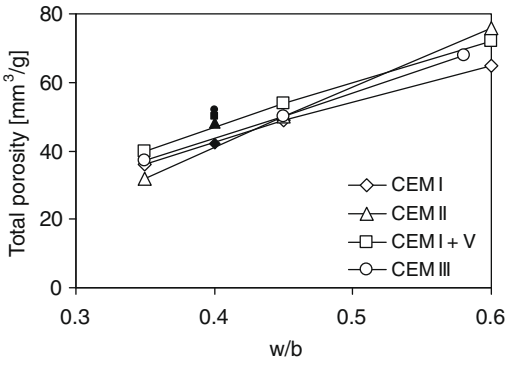

Fig. 1. Total pore volume determined by MIP versus w/b (empty symbols = CVC, filled = SCC).

intrusion curve is shown in Fig. 2 for the mixtures with $w/b = 0.45$. As seen in Fig. 1 total porosity is quite similar for all types of binder, but the pore size distribution for CEM III concrete is shifted to smaller pores compared to the other binders. This applies also to $w/b = 0.35$ and $w/b = 0.60$. The shift of CEM III is more pronounced with increasing w/b.

Pore size distribution of the remaining three binders is quite similar at constant w/b. At $w/b = 0.45$ (Fig. 2) CEM II exhibits only slightly finer pores compared to CEM I and CEM I + V. However, this is not confirmed for w/b 0.35 and 0.60, where the pore size distribution is still very similar but with CEM II having slightly coarser pores. As a consequence the only systematic difference in the MIP intrusion curves is the mentioned shift to smaller pores of CEM III concrete.

As MIP was determined on several small pieces of mortar cut off the concrete, the curves determined by MIP reflect rather the pore size distribution of the mortar than the real porosity in concrete, which includes increased interface porosity along the coarse grains.

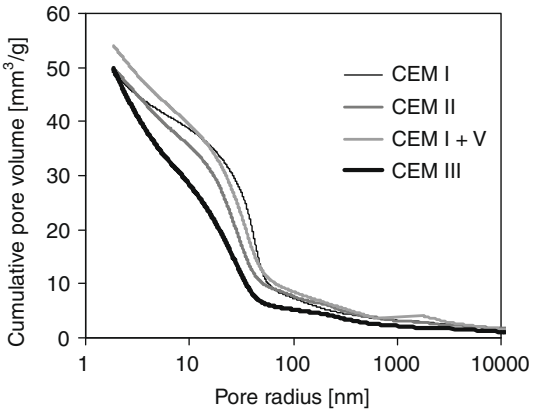

Fig. 2. Cumulative pore volume determined by MIP for the CVC-mixtures with $w/b = 0.45$.

4.3. Chloride resistance

The results measured with the three different methods are plotted in Figs. 3–5 versus compressive strength. This does not mean that strength is the deciding factor for chloride resistance. However, strength class is an important property when designing concrete structures and it is important to know about the relation between compressive strength and chloride resistance. However, as shown in Fig. 1 and described in Chapter 4.1, strength correlates to w/b (mix design) and w/b to porosity, which finally influences the permeability for chloride ingress.

According to all of the three test methods, concrete produced with CEM III has the highest chloride resistance at a given compressive strength. Mixtures with CEM I and CEM I + V are in the same range and display a lower chloride resistance than the mixtures with CEM III. Concrete produced with CEM II displays the lowest chloride resistance as confirmed by all methods.

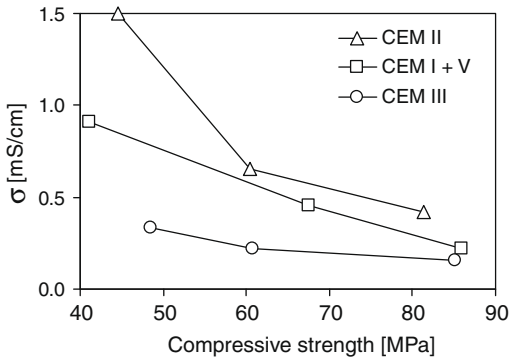

Fig. 3. Conductivity σ versus compressive strength.

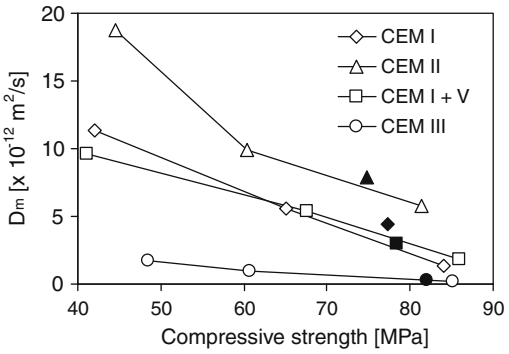

Fig. 4. Chloride migration coefficient D_m versus compressive strength (empty symbols = CVC, filled = SCC).

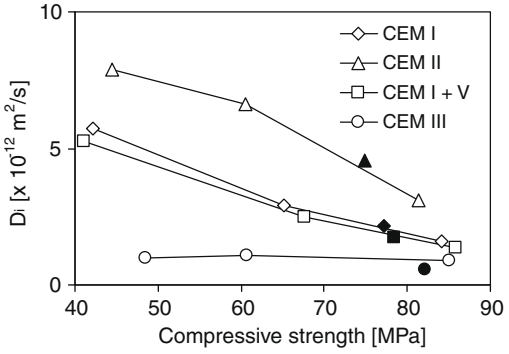

Fig. 5. Apparent chloride diffusion coefficient D_i versus compressive strength (empty symbols = CVC, filled = SCC).

For all of the three methods, chloride resistance is increasing with increasing compressive strength and therefore decreasing with increasing w/b and increasing porosity. As an example, this correlation is shown for migration coefficient D_m in Fig. 6. This correlation is in most cases nearly linear. The decrease of chloride resistance with decreasing compressive strength is higher for the mixtures with CEM II than for the concretes with the other binders. Concrete with CEM III as a binder shows the smallest relation to compressive strength since the measured values are generally very small.

Chloride resistance of the SCC-mixtures is very similar to the one of the corresponding CVC with the same binder. This applies to diffusion coefficient D_i as well as to migration coefficient D_m.

In general, the three methods for testing resistance of concrete to chloride ingress lead to similar results. For all methods the concretes show an increased chloride resistance with increasing compressive strength and the sequence of the different binders is the same for all methods. When comparing the methods to each other, there is a good linear correlation ($R^2 = 0.94$) between migration coefficient D_m and diffusion coefficient D_i for all mixtures including SCC (Fig. 7). However, the intersection point between the correlation line and the D_i-axis and D_m-axis, respectively, in Fig. 7 is not at zero. Therefore D_m seems not to be sensitive enough for very dense concrete. There is also a linear correlation between conductivity σ and D_i (Fig. 8). However, the scatter in this correlation is increased compared to the one in Fig. 7 ($R^2 = 0.83$).

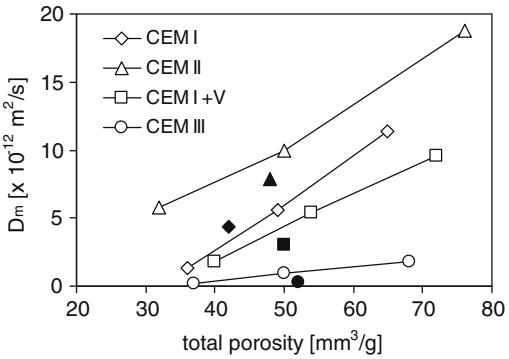

Fig. 6. Migration coefficient D_m versus total porosity determined by MIP.

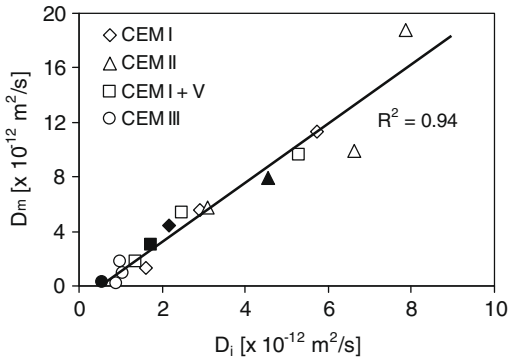

Fig. 7. Migration coefficient D_m versus diffusion coefficient D_i for all mixtures (empty symbols = CVC, filled: SCC).

These correlations are surprising as the measured chloride binding should affect the different test methods used. Diffusion coefficient D_i, which is determined by a slow non-steady-state measurement, should clearly be influenced by chloride binding and conductivity σ, determined by an accelerated steady-state measurement on specimens saturated with chlorides, not at all. Migration coefficient D_m, which is determined also by a non-steady-state test and is additionally, in contrary to diffusion, accelerated by an externally applied electrical field, should show at least a slight influence of chloride binding. As a result, each binder should show a different relation between D_i and the accelerated test methods. However, the correlations obtained imply that the effect of chloride binding is relatively small and cannot explain the differences between the different binders shown in Figs. 3–5.

4.4. Chloride profiles

The profiles of total chloride content in concrete after 50 days immersion out of the test ASTM C 1556 are shown in Fig. 9A for the mixtures with $w/b = 0.45$. All mixtures show a typical decrease of total chloride content with increasing depth from the exposed surface. CEM II shows the highest total chloride content from a

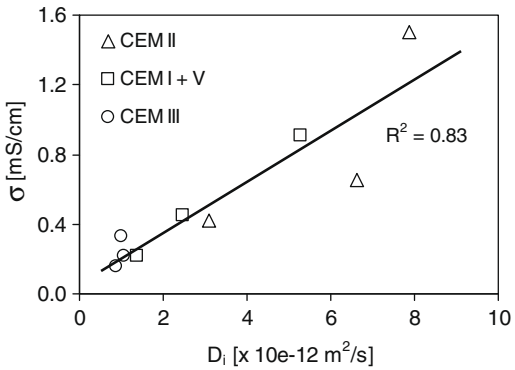

Fig. 8. Conductivity σ versus diffusion coefficient D_i for the measured mixtures.

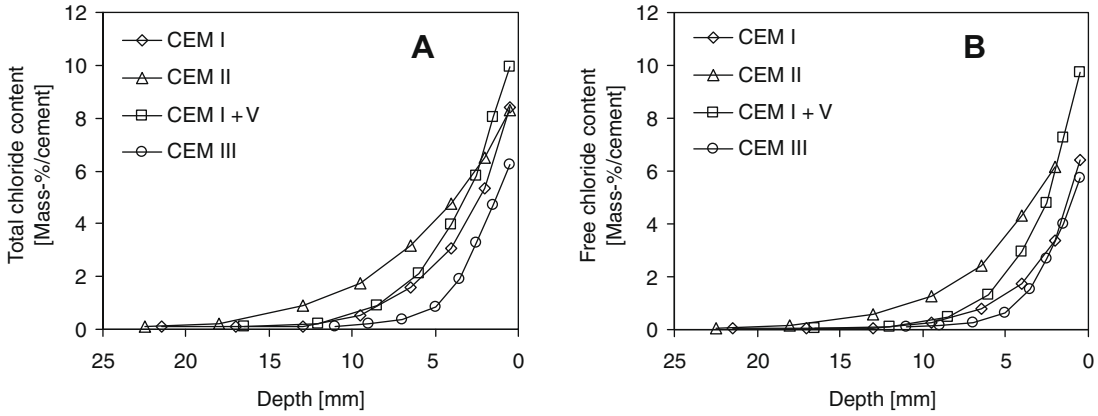

Fig. 9. Profiles of (A) total and (B) free chloride content after 50 days immersion, mixtures with $w/b = 0.45$.

depth of about 3 mm, while CEM III exhibits the lowest total chloride content at any depth. Close to the surface, CEM I + V and CEM I show the highest chloride content. However, with increasing depth, chloride content of CEM I and CEM I + V are decreasing stronger and therefore reach the minimum content at a smaller depth than CEM II. The different depth of chloride indicate the fastest ingress in CEM II and the slowest in CEM III, pointing towards the high chloride resistance for the CEM III cement. As diffusion coefficient D_i was calculated from these profiles, the differences between the chloride profiles of the different binder types agree well with the resistance against chloride ingress found by the diffusion, migration and conductivity test.

Measured profiles of free chloride contents (Fig. 9B) show a similar behavior as the total chloride contents. The free chloride contents are somewhat lower than total chloride contents. However, the difference between total and free chloride content close to the surface is quite small.

The chloride binding for the different binders, calculated as the difference between total and free chloride content, shows some interesting features. The chloride binding for CEM I is independent from w/b and volume of paste (Fig. 10), which was confirmed by other authors [4,28]. It is dependent on the chloride concentration in the pores only. Therefore, measured chloride binding has no direct effect on the increased chloride resistance with increasing compressive strength and decreasing w/b, but is in agreement with the comparable chloride resistance between SCC and CVC at constant compressive strength.

Plotting the chloride fraction bound against the total chloride content (Fig. 11), concrete produced with CEM III shows the lowest chloride binding. For CEM II, chloride binding is also lower compared to CEM I + V and CEM I, which exhibits the highest fraction of bound chlorides. A lower chloride binding capacity of OPC blended with slag compared to plain OPC was also obtained by some other authors (e.g. Mohammed et al. [29]), while many other studies found the opposite. Based on the chemical composition, CEM III is expected to have the highest ability to bind chlorides by forming Friedel's salt due to its high Al_2O_3 to SO_3 ratio (see Table 1). A high Al_2O_3/SO_3 ratio will lead to the formation of more AFm phases and less AFt phases and thus increase the potential of the cement to form Friedels salt. Jones et al. [3] could show that blending OPC with mineral admixtures such as blast furnace slag or fly ash increases the ratio of AFm to AFt and, thereby, greatly increases the potential sites for chloride binding. In agreement with these observations, Arya et al. [30] or Luo et al. [31] found also an increased chloride binding for OPC blended with blast furnace slag. Note that in these studies, chloride was added during mixing.

Therefore the low observed chloride binding of CEM III seems at first glance somewhat surprising, considering the chemical composition and very small ingress of chloride in Fig. 9A. These findings indicate again, that chloride binding seems not to be the main factor that determines the speed of chloride ingress.

Additionally, the maximum in bound chloride content in Fig. 11 is for all binders not at the highest total chloride content. This phenomenon will be discussed in the following section.

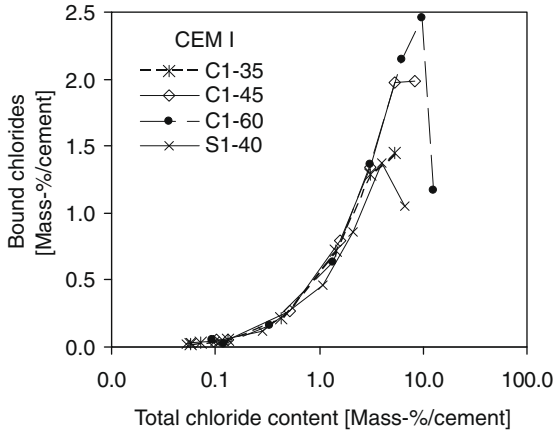

Fig. 10. Bound chloride content versus total chloride content for CEM I mixtures with different w/b.

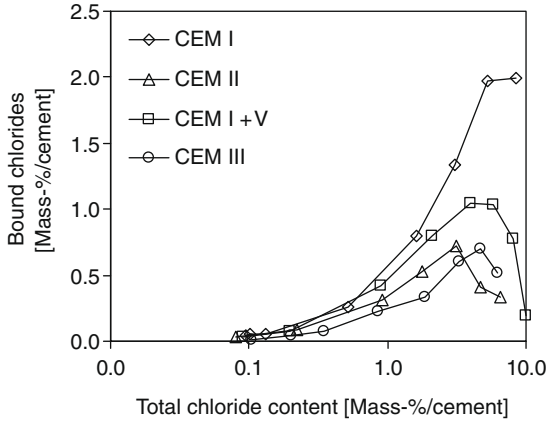

Fig. 11. Bound chloride content versus total chloride content for different binders with $w/b = 0.45$.

4.5. Thermodynamic modeling

Thermodynamic modeling can be used to calculate the potential of different cements to bind chloride in Friedel's salt $Ca_4Al_2Cl_2(OH)_{12}\cdot 4H_2O$. In the present calculations, the influence of chloride binding on C–S–H has been neglected, as in most OPC the influence of the Al-containing phases is much more important [32] and as in all cements studied similar amounts of C–S–H are present.

The unaffected core of the CEM I sample after 62 days in saturated calcium hydroxide solution is calculated to consist mainly of C–S–H, portlandite, ettringite and monocarbonate, with smaller quantities of calcite, hydrotalcite, $Fe(OH)_3$ and unhydrated clinker (Fig. 12A). The ingression of NaCl was mimicked in these calculations assuming that the core of the sample is in contact with no additional solution containing NaCl, while the area near the surface is in contact with large quantities of solution. Upon the ingression of NaCl, thermodynamics predicts the transformation of monocarbonate to Friedel's salt and calcite. Near to the surface in the presence of high chloride concentrations, even ettringite and portlandite become unstable and even more Friedel's salt is formed. At the surface of the sample portlandite, also C–S–H and the Friedel's salt are leached by the NaCl solution. This sequence agrees with the experimental observations in this study (decreasing chloride binding in Fig. 11 at high total chloride content) and in the literature: a decrease of the mass% of chloride, calcium, sulfate and silicon [33] as well as a depletion of Friedels salt and portlandite [34] was observed near the surface of paste samples exposed to NaCl solutions.

Similarly to the CEM I sample, the unaffected core of the CEM III sample after 62 days in saturated calcium hydroxide solution is composed of C–S–H, portlandite, ettringite and monocarbonate (Fig. 12B). Beside unhydrated clinker, a significant fraction of the slag is expected to remain unhydrated, in agreement with the findings in studies concerning the degree of hydration of slag cements. Escalante et al. [35] found a degree of hydration of 20–50% for slag, dependent on hydration temperature, w/b ratio and replacement level. Lumley et al. [36] describe also a dependence of degree of slag hydration from w/b and replacement level leading to degrees of hydration between 30 and 55% after 28 days and 45–75% after 1–2 years. Beside slag, also for fly ash very limited degrees of hydration have been found [37].

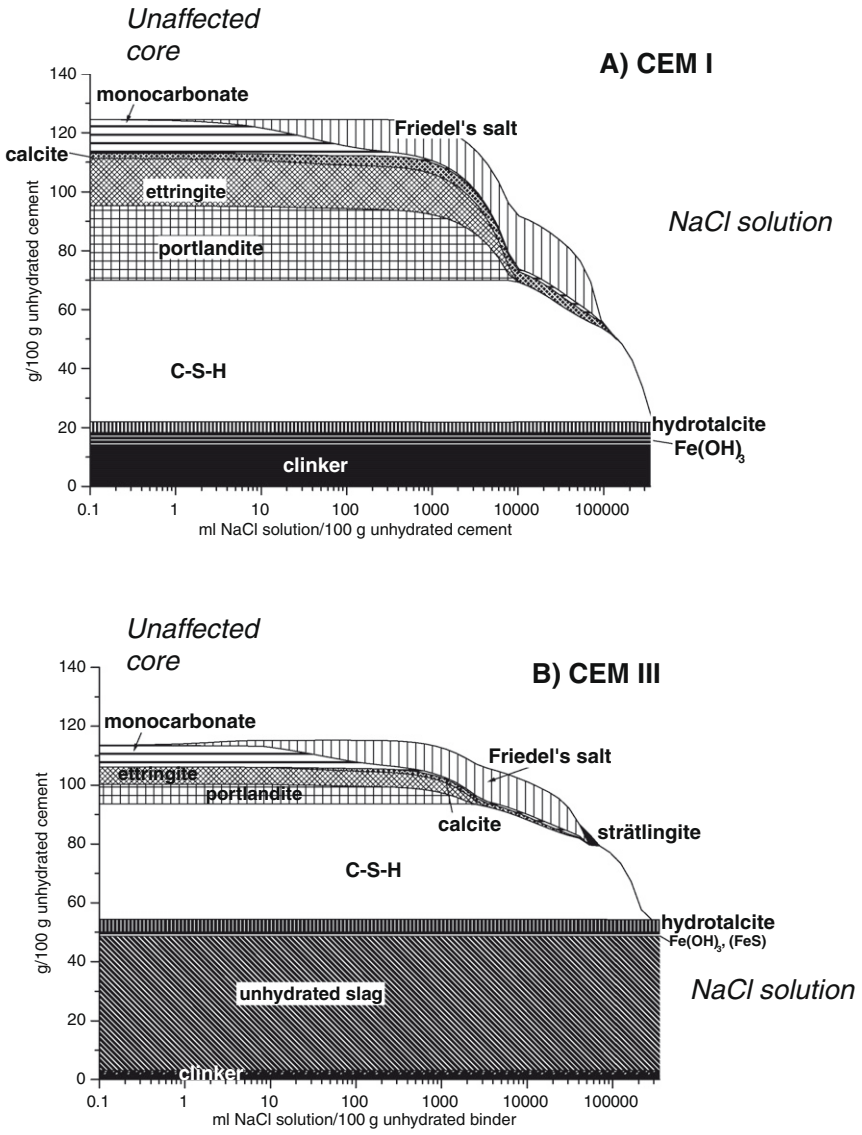

Fig. 12. Calculated phase assemblage in (A) the CEM I and (B) CEM III sample subjected to NaCl solutions (165 g NaCl/l). In the core of the sample, basically no additional NaCl solution is present, while the binder directly at the surface is in contact with a relatively large volume of NaCl solution.

Based on these findings for the present calculation it was assumed that 30% of the slag had reacted. Again, the monocarbonate present is calculated to become unstable with respect to Friedel's salt and calcite. Near the surface first portlandite and ettringite become unstable. Even nearer to the surface also Friedel's salt and the C–S–H phases will become unstable.

The total chloride uptake in the solid phase of the four different cements was calculated and expressed as g chloride per 100 g unhydrated cement. For CEM I a maximum uptake of 2.3 g Cl/100 g cement was calculated (Fig. 13), which agrees well with the measured uptake as given in Fig. 10.

The Portland limestone cement CEM II, which contains approx. 14% of limestone, exhibits the same hydration products as the CEM I, but contains somewhat less aluminum (see Table 1). Thus, the CEM II has a lower potential to form Friedel's salt and is predicted to exhibit a lower chloride uptake than the CEM I cement (Fig. 13), which is in agreement with the experimental data presented in Fig. 11.

Similar to the replacement of OPC with limestone, also the blending of OPC with slag or fly ash can lower the chloride binding capacity. Even if these replacement materials contain significant amounts of aluminum (as e.g. the low Ca-fly ash used in this study, Table 1), the aluminum is only available to form Friedel's salt to the extent that the mineral admixture has reacted. The data for CEM III and CEM I + V presented in Fig. 13, correspond to the assumption that after 63 days 30% of the slag and 5% of the fly ash have reacted. Under these conditions, a clearly lower potential of the blended materials for chloride binding has been calculated (see Fig. 13), which agrees well with the experimental findings as represented in Fig. 11. If a higher fraction of these mineral admixtures had reacted, however, these cements would exhibit a higher chloride binding. Therefore, the assumed degree of hydration of the slag could also be a possible reason for the difference between measured and modeled amount of bound chlorides in case of CEM II and CEM III.

In the investigation presented here, the use of supplementary cementitious materials lowers the capacity to bind chloride in the cement. Similarly to our results, Zibara [28] observed in his thesis at a w/c of 0.3 partially a reduction of chloride uptake in the presence of fly ash. At a w/c of 0.5, however, he observed in all cases an increase of chloride uptake, even though the effect of different fly ashes was very different. Most authors reported (see Tables 2–1 in [28]) an increase of chloride binding upon the blending with fly ash while only very few reported a decrease. Such a divers influence of fly ash is to be expected as different fly ashes exhibit very different reactivities. The situation is similar for slags, where the reactivity of the slag also depends strongly on the composition and the fineness of slag. This indicates, that whether the addition of slag or fly ash will increase chloride uptake or not will depend to large extent on the reactivity of mineral admixture used.

5. Conclusions

For a given binder there is a nearly linear correlation between total porosity determined by MIP and the chloride resistance determined by all methods considered. It can be concluded, that for a given binder, total porosity is the most important factor influencing chloride resistance. However, this relation differs from binder to binder. While concrete produced with slag cement (CEM III/A) has a considerably higher chloride resistance than concrete produced with CEM I and CEM I with fly ash, which have a comparable chloride resistance, mixtures with Portland limestone cement CEM II/A-LL show the lowest chloride resistance. MIP indicates that the higher chloride resistance of concrete produced with CEM III is due to its finer pore size distribution. As the pore size distribution of concrete produced with the other three cements is nearly identical, MIP can give no explanation for the differences in chloride resistance. As reported in [38], also differences in the interfacial transition zone (ITZ) due to the different binders, which would affect the penetration of the chlorides, are not expected. Therefore, the reason for the differences in chloride resistance is expected to be binder specific pore characteristics like tortuosity that are not reflected in MIP. Other methods like nitrogen adsorption or microscopic methods may be able to better show the connection of pore characteristics and permeability.

Chemical parameters have a certain influence on chloride resistance as well. But in all investigated cases, only a limited fraction of chloride is bound by the cement while the larger fraction is in the solution. This applies also to binders, whose chemical composition imply a high potential for forming Friedel's salt. This is a result of the different reactivities of the different mineral admixtures as it can be shown by thermodynamic modeling. Only a relatively small fraction of the fly ash and of the slag present have reacted, result-

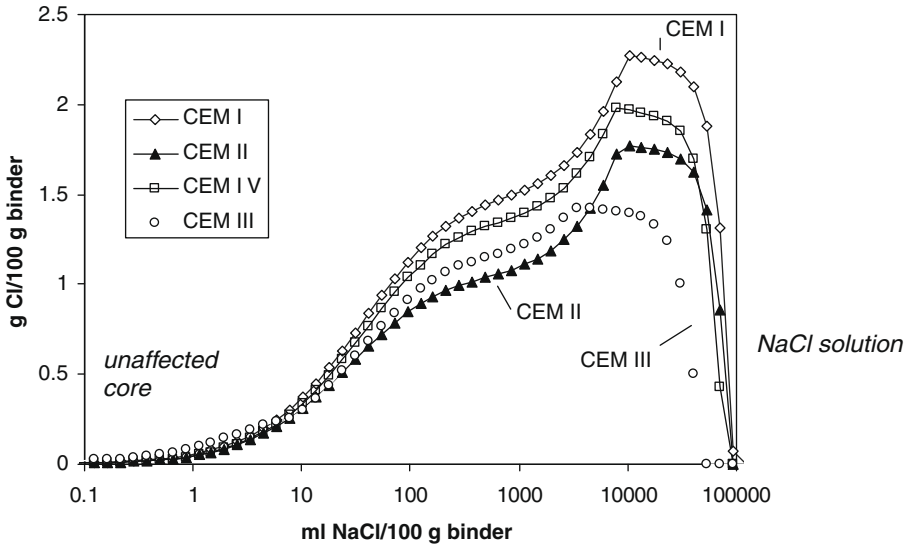

Fig. 13. Calculated bound chloride for different binder systems subjected to NaCl solutions (165 g NaCl/l). In the core of the sample, basically no additional NaCl solution is present, while the binder directly at the surface is in contact with a relatively large volume of NaCl solution.

ing in little additional aluminum that is available to form Friedel's salt. The aluminum still present in the unreacted fraction of slag or fly ash will obviously not increase the chloride binding. Thus the effect of binding on chloride ingression is less important compared to the effect of permeability. This fact can be illustrated by the good correlation between diffusion coefficient, migration coefficient (Fig. 7) and conductivity (Fig. 8), respectively. If chloride binding would affect the results significantly, there would not be a good correlation between the different methods as they are influenced differently by chloride binding.

Acknowledgements

The authors would like to address their thanks to Josef Kaufmann for the MIP-measurements and to Ronald Lay for the determination of the chloride profiles.

References

[1] Neville AM. Effects of freezing and thawing and of chlorides. In: Properties of concrete. Longman, Essex; 1995.
[2] Guettala A, Abibsi A. Corrosion degradation and repair of a concrete bridge. Mater Struct 2006;39:471–8.
[3] Jones MR et al. Studies using 27Al MAS NMR of AFm and AFt phases and the formation of Friedel's salt. Cem Concr Res 2003;33:177–82.
[4] Tang L, Nilsson LO. Chloride binding capacity and binding isotherms of OPC pastes and mortars. Cem Concr Res 1992;23:247–53.
[5] Sandberg P. Studies of chloride binding in concrete exposed in marine environment. Cem Concr Res 1999;29:473–7.
[6] Geiker M, Nielsen EP, Herfort D. Prediction of chloride ingress and binding in cement paste. Mater Struct 2007;40:405–17.
[7] Samson E, Marchand J. Modeling the effect of temperature on ionic transport in cementitious materials. Cem Concr Res 2007;37:455–68.
[8] Yang CC. On the relationship between pore structure and chloride diffusivity from accelerated chloride migration test in cement-based materials. Cem Concr Res 2006;36:1304–10.
[9] Costa A, Appleton J. Chloride penetration into concrete in marine environment – part I: main parameters affecting chloride penetration. Mater Struct 1999;32:252–9.
[10] CHLORTEST. Resistance of concrete to chloride ingress – from laboratory tests to infield performance. EU-Project (5th FP GROWTH) G6RD-CT-2002-00855, WP2, report: pre-evaluation of different test methods; 2005.
[11] Stanish KD, Hooton RD, Thomas MDA. Testing the chloride penetration resistance of concrete: a literature review. FHWA contract DTFH61-97-R-00022. Prediction of chloride penetration in concrete; 1997.
[12] Tang L. Chloride transport in concrete – measurement and prediction. PhD thesis, publication P-96:6. Dept. of Building Materials, Chalmers University of Technology, Gothenburg, Sweden; 1996.
[13] EN 197-1. Cement – part 1: composition, specifications and conformity criteria for common cements; 2000.
[14] Skarendal A, Petersson Ö. Self-compacting concrete. State-of-the-art report of RILEM technical committee 174-SCC. Report 23; 2000.
[15] EN 12350-5. Testing fresh concrete – part 5: flow table test; 2001.
[16] EN 12390-3. Testing hardened concrete – part 3: compressive strength of test specimens; 2002.
[17] American Society for Testing and Materials (ASTM). Standard test method for determining the apparent chloride diffusion coefficient of cementitious mixtures by bulk diffusion. Code ASTM C 1556; 2003.
[18] Schweizer Ingenieur- und Architektenverein. Concrete structures – Supplementary specifications, Appendix B: chloride resistance. Swiss standard 505, no. 262/1; 2003.
[19] Alexander MG, Streicher PE, Mackechnie JR. Rapid chloride conductivity testing of concrete. Research monograph no. 3. Department of Civil Engineering, University of Cape Town; 1999.
[20] EN 14629. Products and systems for the protection and repair of concrete structures – test methods – determination of chloride content in hardened concrete; 2007.
[21] RILEM TC 178-TMC. Round-Robin test on chloride analysis in concrete – part II: analysis of water soluble chloride content. Mater Struct 2001;34:589–98.
[22] Kulik D. GEMS-PSI 2.2. PSI-Villigen, Switzerland; 2007. <http://gems.web.psi.ch/>.
[23] Thoenen T, Kulik D. Nagra/PSI chemical thermodynamic database 01/01 for the GEM-Selektor (V.2-PSI) geochemical modeling code, PSI, Villigen; 2003. <http://gems.web.psi.ch/doc/pdf/TM-44-03-04-web.pdf>.
[24] Hummel W, Berner U, Curti E, Pearson FJ, Thoenen T. Nagra/PSI Chemical thermodynamic data base 01/01. USA: Universal Publishers; 2002. <uPUBLISH.com>.
[25] Lothenbach B, Matschei T, Möschner G, Glasser FP. Thermodynamic modeling of the effect of temperature on the hydration and porosity of Portland cement. Cem Concr Res 2008;38:1–18.
[26] Lothenbach B, Le Saout G, Gallucci E, Scrivener K. Influence of limestone on the hydration of Portland cements. Cem Concr Res 2008;38:848–60.
[27] Hobbs MY. Solubilities and ion exchange properties of solid solutions between OH, Cl and CO_3 end members of the monocalcium aluminate hydrates. PhD thesis, University of Waterloo, Ontario, Canada; 2001.
[28] Zibara H. Binding of external chlorides by cement pastes. PhD thesis, University of Toronto, Canada; 2001.
[29] Mohammed TU, Hamada H. Relationship between free chloride and total chloride contents in concrete. Cem Concr Res 2003;33:1487–90.
[30] Arya C, Xu Y. Effect of cement type on chloride binding and corrosion of steel in concrete. Cem Concr Res 1995;25:893–902.
[31] Luo R et al. Study of chloride binding and diffusion in GGBS concrete. Cem Concr Res 2003;33:1–7.
[32] Zibara H, Hooton D, Yamada K, Thomas MDA. Roles of cement mineral phases in chloride binding. Cem Sci Concr Technol 2002;56:384–91.
[33] Johannesson B, Yamada K, Nilsson LO, Hosokawa Y. Multi-species ionic diffusion in concrete with account to interaction between ions in the pore solution and the cement hydrates. Mater Struct 2007;40:651–65.
[34] Sugiyama T, Ritthichauy W, Tsuji Y. Experimental investigation and numerical modeling of chloride penetration and calcium dissolution in saturated concrete. Cem Concr Res 2008;38:49–67.
[35] Escalante JI et al. Reactivity of blast-furnace slag in Portland cement blends hydrated under different conditions. Cem Concr Res 2001;31:1403–9.
[36] Lumley JS, Gollop RS, Moir GK, Taylor HFW. Degrees of reaction of slag in some blends with Portland cements. Cem Concr Res 1996;26:139–51.
[37] Lam L, Wong YL, Poon CS. Degree of hydration and gel/space ratio of high-volume fly ash/cement systems. Cem Concr Res 2000;30:747–56.
[38] Leemann A, Loser R, Münch B. Influence of cement type on the porosity in the interfacial transition zone of self-compacting concrete. Cem Concr Comp, 2009, submitted for publication.